

# High-energy $\gamma$ -rays in $\alpha$ -accompanied spontaneous fission of $^{252}\text{Cf}$

P. Singer<sup>1</sup>, M. Mutterer<sup>1</sup>, Yu. N. Kopach<sup>2</sup>, M. Klemens<sup>1</sup>, A. Hotzel<sup>3,\*</sup>, D. Schwalm<sup>3</sup>, P. Thierolf<sup>3,\*\*</sup>, M. Hesse<sup>4</sup>

<sup>1</sup> Institut für Kernphysik, Technische Hochschule, D-64289 Darmstadt, Germany

<sup>2</sup> Frank Laboratory of Neutron Physics, JINR, Dubna, Russia

<sup>3</sup> Max-Planck-Institut für Kernphysik, D-69115 Heidelberg, Germany

<sup>4</sup> Physikalisches Institut der Universität, D-72076 Tübingen, Germany

Received: 18 March 1997

Communicated by B. Povh

**Abstract.** An experiment was performed on prompt  $\gamma$ -ray emission in binary and  $\alpha$ -particle accompanied spontaneous fission of  $^{252}\text{Cf}$  using the Darmstadt-Heidelberg  $4\pi \text{NaI}$  Crystal Ball spectrometer. The enhancement in  $\gamma$ -ray yield, denoted as the “high-energy component”, which appears between 3.5 and 8 MeV and in the region of near-symmetric fragment mass splits, was observed to be equally pronounced in both fission modes. Analyzing the fragment mass dependence of the mean  $\gamma$ -ray multiplicity in both fission modes clearly identifies the disintegration of equilibrated fission fragments in a narrow mass range around the double-magic  $^{132}\text{Sn}$  as the source of these  $\gamma$ -rays.

**PACS:** 25.85.Ca; 23.20.Lv

## 1 Introduction

The study of  $\gamma$ -ray emission in fission is of great interest as it allows probing fragment excitation energies and spins after neutron evaporation as well as fragment level schemes and, thus, collective and single-particle aspects of nuclei far from stability [1]. The gross structure of the prompt fission  $\gamma$ -ray spectrum, in a wide interval from 1 MeV to 8 MeV, is characterized by the exponentially decreasing yield of statistical  $\gamma$ -rays (mainly  $E1$  transitions) which come first in the  $\gamma$  cascade. At energies below 1 MeV, the subsequent emission of discrete  $\gamma$ -rays along the Yrast sequence of rotating fragments dominates the spectrum and, at energies higher than 8 MeV, the onset of the GDR leads to a slight enhancement. A striking exception to this general shape was found recently in the spontaneous fission of  $^{252}\text{Cf}$  [2]. A pronounced enhancement in the  $\gamma$  spectrum was observed between 3 and 8 MeV, which appeared only in the narrow region of near-symmetric fragment mass splits. At that time, it was unclear whether the source of this particular  $\gamma$ -ray bump is a peculiarity in the de-excitation

of equilibrated fragments or is rather of a collective nature due to the rotational and translational motion of nuclear matter near scission or in an early phase of fragment acceleration [3, 4].

The “high-energy  $\gamma$ -ray component” in question has been studied extensively during the last couple of years, predominantly in experiments performed at MPI Heidelberg, using the Darmstadt-Heidelberg Crystal Ball (CB) spectrometer as a highly effective  $\gamma$ -ray detector. Gamma rays from both fragments were registered in  $4\pi$  geometry, in coincidence with the fission fragments from each fission event. Different methods were applied to identify which nuclei among the fragments are the source of this unusual enhancement of the  $\gamma$ -ray yield. In [5], a series of fusion-fission reactions leading to different compound nuclei were studied and, in a recent CB experiment on  $^{252}\text{Cf}$  [6], the mass assignment of the surplus high-energy  $\gamma$ -rays was achieved by analyzing the “effective” velocities of fragment pairs by means of the Doppler effect, taking advantage of angle-sensitive detection of the fragments and the  $\gamma$ -rays. Both experiments conform with an emission from equilibrated fragments with masses in the vicinity of the spherical shell closures at  $Z = 50$  and  $N = 82$ . For  $^{252}\text{Cf}$  the measured spectral shape and the distribution of the  $\gamma$ -ray yield as a function of mass could be simulated rather well by a statistical model calculation where mass-dependent level density parameters [7], as empirically deduced from fission neutron spectra of  $^{252}\text{Cf}$ , were taken as the input [6].

The measurement of prompt  $\gamma$ -rays in particle-accompanied fission provides another method for investigating the origin of these  $\gamma$ 's [8]. In this relatively rare process, described also as ternary fission, a light charged particle (LCP, in 90% of the cases an  $\alpha$  particle) is emitted from the neck region of the separating nuclei during scission [9, 10]. In this case, the number of nucleons available for forming the fission fragments is reduced by the LCP mass. Thus, a comparison of the measured  $\gamma$ -ray yields in binary and  $\alpha$ -particle-accompanied fission versus fragment mass allows one to identify unambiguously whether the light or heavy fragment of the fission event is emitting the  $\gamma$ -rays in question. In the present work, the proper experimental conditions of good statistics and fragment mass resolution for such an analysis were met for the first time.

\* present address: Fritz-Haber-Institut der MPG, D-14195 Berlin, Germany

\*\* present address: Ludwig-Maximilian-Universität München, D-85748 Garching, Germany

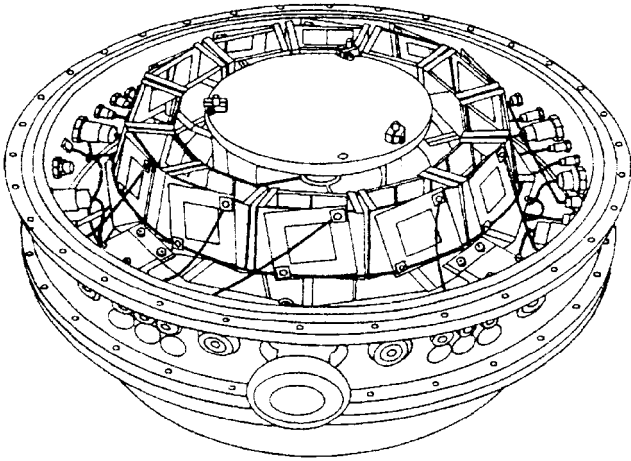


**Fig. 1.** Schematic view of the CODIS detection system. The upper part of the vessel (30 cm in diameter) is removed to have a view onto the ring of 12  $\Delta E$ -E telescopes, arranged around one half of the double ionization chamber. All detectors were operated in  $CH_4$  atmosphere at  $0.75 \times 10^5$  Pa

## 2 Experiment

The experiment was again performed at the Darmstadt-Heidelberg Crystal Ball spectrometer. This instrument is a segmented  $4\pi$  detection system with high efficiency and granularity, consisting of a dense spherical package of 162  $NaI(Tl)$  crystals [11]. The  $^{252}Cf$  sample and the assembly of detectors for the fragments and ternary particles were mounted inside of the hollow sphere 50 cm in diameter at the center of the crystal ball. This CODIS detection system (see Fig. 1) is composed of two different devices assembled in a common near-spherical vessel 30 cm in diameter, filled with  $CH_4$  at  $0.75 \times 10^5$  Pa as the counting gas [12].

A Frisch-gridded  $4\pi$  twin ionization chamber (IC) measures the fragment energies and their angles of emission from the central source. Determination of the angles is achieved by measuring the electron drift times in both grid-cathode spaces (for the azimuthal angles) and by means of a common segmented cathode plate (for both the azimuthal and polar angles) similar to that used in [6, 13]. In our case, four quadrants of angle-sensing electrodes, with an outer radius of 34 mm, were etched onto both sides of the cathode plate made of copper-plated teflon material. This geometry of electrodes and the low dielectric constant of teflon minimizes the capacitive interference between fast signals from both sides of the cathode. The central part of the cathode, which is essentially the metallized source holder and backing 22 mm in diameter (having a central part of  $30 \mu g/cm^2$   $Al_2O_3$  with  $10 \mu g/cm^2$   $Au$  on both sides supporting the sample spot of 5 mm diameter) is used to derive the event trigger for all detectors, with a time resolution of  $\leq 1.5$  ns fwhm. Fragment energy signals were derived from the chamber anodes. Since we used a rather active  $^{252}Cf$  source with  $4 \times 10^3$  fissions/s, which provides also a 30 times higher rate of 6.1 MeV  $\alpha$ -particles from radioactive decay, we took precautions to avoid pulse distortions due to pile-up. The energy signals from the anodes of both halves of the chamber were derived by current-sensitive preamplifiers fed into QDCs with an integration time of 1  $\mu s$ , and electronic pile-up rejection was performed with fast timing signals from the preamplifiers, with a pulse-pair resolution of 200 ns. The

residual pile-up could be reduced to a level of 2% for the  $\alpha$ -particle-fragment pile-up, and to 0.1% for pile-up between fragment pulses.

Light charged particles from ternary fission were measured by a ring of 12  $\Delta E$ -E telescopes composed of small  $\Delta E$  ICs and silicon PIN diodes surrounding one half of the fragment IC, at a distance of 10.2 cm between the PIN diodes and the source. Residual energies of the LCPs were registered by the  $30 \times 30$  mm<sup>2</sup> and 380  $\mu m$  thick silicon PIN diodes. Energy-loss signals for particle identification were obtained from the small Frisch-grid ICs that used the PIN diode surfaces as the cathodes. Anodes of these small ICs were made from thin plastic foils, with metallic layers evaporated onto them in a way to further subdivide each anode surface into four quadrants. The size of these quadrants ( $14 \times 14$  mm<sup>2</sup>) defines the emission angle of the ternary particles within a resolution of  $\pm 5^\circ$  fwhm. The  $\Delta E$  resolution of the telescope ICs was sufficient to separate ternary  $\alpha$ -particles from other LCP species ( $^3H$ ,  $^6,8He$ ,  $Li$ ,  $Be$ ,  $B$ , and  $C$ ) observed [12].

During a four-week run, we registered  $1.2 \times 10^6$  ternary fission events accompanied by  $\alpha$ -particles. Simultaneously,  $7 \times 10^7$  binary fission events were recorded. For the binary events, coincident response of the CB was required, for the ternary ones also a fast timing signal from one of the 12 PIN diodes. Since the probability for  $\alpha$ -particle accompanied fission is only  $\approx 1/300$  and the total solid angle subtended by the telescopes is small (about  $\pi/4$ ), data rates for both fission modes were different by a factor of  $\approx 1/4000$ . The acquisition rate of binary fission data was therefore reduced by a factor of  $1/64$ .

With the CB, clean separation of  $\gamma$ -ray pulses from the delayed pulses of fission neutrons is achieved by exploiting the fast timing signals from each individual module [6]. Pulse-height calibration of the CB was performed with various  $\gamma$ -ray sources, using standard procedures. Unfolding of the measured  $\gamma$  spectra from the detector response function was not performed because the deconvolution procedure can produce systematic errors, especially in domains with weak statistics. Thus, energy distributions discussed in the present paper refer to calibrated pulse-height distributions. However, differences in the  $\gamma$  efficiency between the individual detectors were corrected using information derived from the experiment itself. No summing corrections, accounting for the probability of double hits from  $\gamma$ -rays and neutrons coming from the same fission event, were applied because this effect significantly deteriorates the spectrum only at the highest energies,  $E_\gamma \geq 7$  MeV [13].

## 3 Results and discussion

### 3.1 Characteristics of $\alpha$ -particle accompanied fission

The energy spectrum of the ternary  $\alpha$ -particles is depicted in Fig. 2a. Due to the absorption in the chamber gas and the foils, only  $\alpha$ -particles with energies above 8 MeV reach the PIN diodes. The first and second moments (15.7 MeV and 11.2 MeV fwhm, respectively) of the energy distribution are in close agreement with data from the literature [14]. Also, the measured distribution of emission angles ( $83.9^\circ$  and

20.9° fwhm for the first and second moments, respectively), relative to the direction of the light group of fission fragments, coincides with known data [14], proving the quality of our angle determinations. Energy and mass spectra of primary fission fragments, i.e. prior to neutron evaporation, are shown in Figs. 2b,c for fission events measured in coincidence with these  $\alpha$ -particles and compared to the spectra evaluated for binary fission. Fragment masses were deduced from the ratio of measured kinetic energies of the fission fragments for each event, after having made mass, energy, and emission-angle dependent corrections for the pulse-height defect and for the energy loss in the target and the backing, and a correction for prompt neutron evaporation. The spectra for binary fission were evaluated as in [6], using data on mean fragment energies from [15] as the reference. The correction for the evaporation of neutrons was performed with applying data from [16] on mean neutron multiplicities versus fragment mass and total kinetic energy  $TKE$ . In the analysis of the fragment mass splits in ternary fission, the recoil correction for the emission of the ternary particle was performed. Here, emission of prompt neutrons was corrected as function of mass, employing data from [17].

Our mass determination and the achieved resolution were ascertained experimentally by means of the  $^{134}\text{Te}$  isotope. This isotope is formed in an isomeric state which decays, with a half-life of 160 ns, via a  $3\gamma$  cascade with energies of 115 keV, 297 keV, and 1280 keV, respectively. Gating a triple fast-slow coincidence on these energies, with the condition of a common delay of  $\geq 100$  ns relative to the prompt trigger, has yielded a mass spectrum with a single heavy-fragment mass line at the positions of  $A_H = 135.3 \pm 0.5$  and  $A_H = 135.4 \pm 0.4$  mass units for the binary and ternary cases, respectively. These locations agree with  $A = 134$ , considering that evaporation of 1.2 neutrons, on average, precedes the formation of  $^{134}\text{Te}$  [18]. The experimental mass resolution, deduced from the widths of the  $^{134}\text{Te}$  peaks, was found to be  $3.9 \pm 0.6$  ( $4.9 \pm 0.6$ ) units fwhm for binary ( $\alpha$ -accompanied) fission. The fragment mass resolution in the present experiment is close to the estimated limit of 3.9 units for the double-energy method [19] and, thus, is caused mainly by neutron emission broadening.

The similarity of the fragment spectra in Figs. 2b,c shows that both fission modes yield fragments which are very similar in their excitation characteristics. It is known from [12, 14] that the mean total excitation energy  $TXE$  of 35 MeV of the  $^{252}\text{Cf}$  fragments is reduced by about 20% in the  $\alpha$ -accompanied fission mode, which is also manifested in the reduction of the mean number of neutrons per fission  $\bar{\nu}$  from 3.77 to 3.08. The remaining energies for  $\gamma$ -ray emission in the late stages of the decay chains should, therefore, be rather close to each other.

### 3.2 Gamma-ray spectra and multiplicities

The energy spectra of  $\gamma$ -rays observed in both fission modes are shown in Fig. 3 for two different mass intervals as examples. The spectra were normalized according to the number of fission events recorded with the respective mass splits. Within the range of heavy-fragment masses  $126 \leq A_H \leq 136$  near the mass symmetry, the pronounced high-energy component between 3.5 and 8 MeV shows up in ternary as well as in binary fission. Figure 4 represents the mean  $\gamma$ -ray multiplicity in

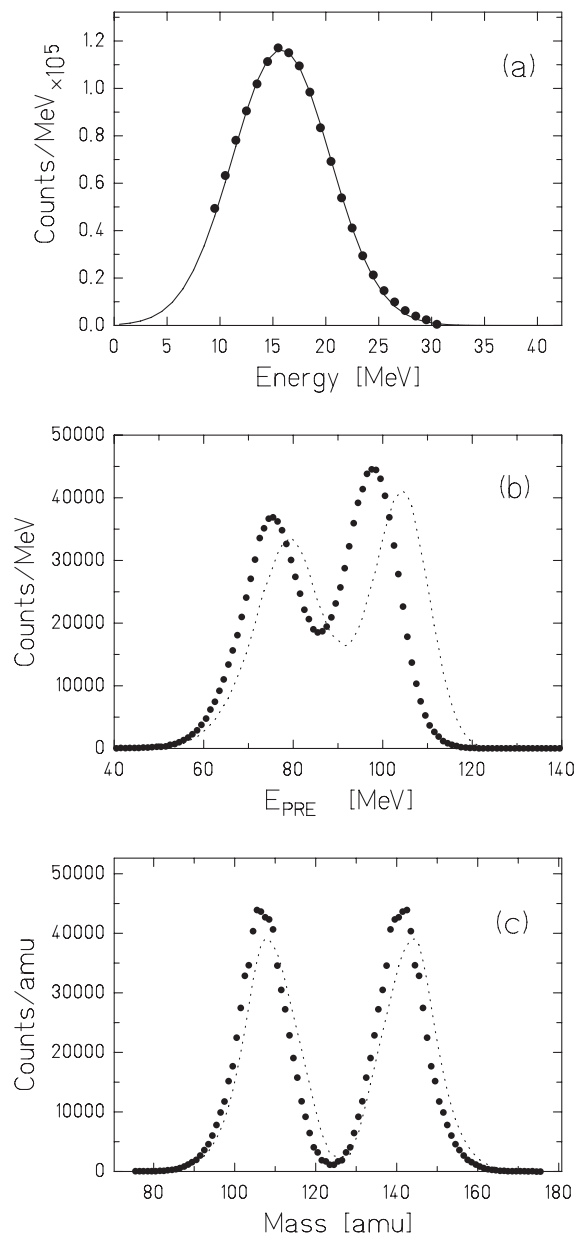


**Fig. 2.** **a** Energy spectrum of ternary  $\alpha$ -particles. **b** Fragment (pre-neutron) energy distribution, and **c** fragment (pre-neutron) mass distribution, in coincidence with ternary  $\alpha$ -particles. The full line in **a** is a Gaussian fit. Dotted lines in **b,c** show the corresponding spectra for binary fission events, normalized to the same area

the  $\gamma$ -energy range from 4 to 8 MeV, as a function of fragment mass. Since the CB measures total  $\gamma$ -ray multiplicity per mass split, the structures in the multiplicity distributions shown are mirrored at the respective positions of mass symmetry. The distribution related to binary fission is in close agreement with the result of the previous CB experiment [6]. In the  $\alpha$ -particle accompanied fission mode, unlike the binary case, the observed peak around  $A = 131$  is clearly resolved from its counterpart located at the complementary light mass, since the sum of the fragment mass numbers is reduced by 4 units compared to binary fission. The peaks at the heavy masses are very close to each other. Fitting of Gaussian curves to the data has yielded peak positions at  $A = 131.1 \pm 0.3$  ( $A = 130.5 \pm 0.1$ ) units

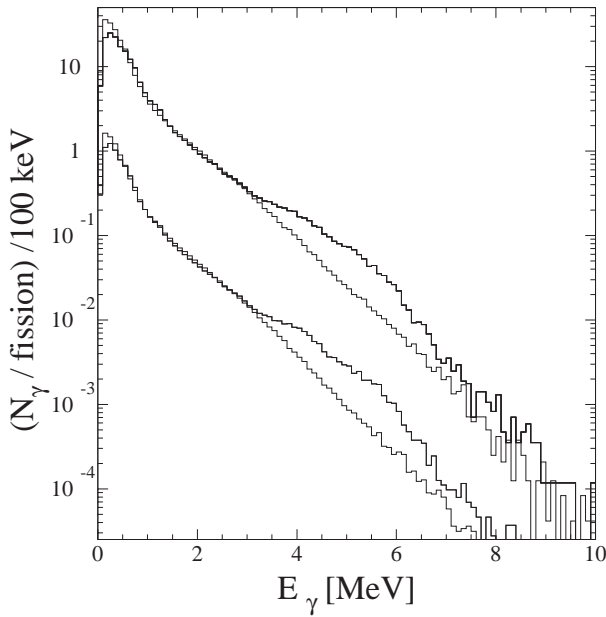


**Fig. 3.** Energy spectra of  $\gamma$ -rays for binary (upper curves) and  $\alpha$ -accompanied (lower curves) fission, for fragment mass splits with  $126 \leq A_H \leq 136$  (full lines), and  $144 \leq A_H \leq 154$  (dotted lines), respectively. The corresponding light-fragment masses are  $116 \leq A_L \leq 126$  ( $112 \leq A_L \leq 122$ ) and  $98 \leq A_L \leq 108$  ( $94 \leq A_L \leq 104$ ), respectively, for binary ( $\alpha$ -accompanied) fission. The binary spectra, containing  $1.2 \times 10^6$  fission events total (as measured for  $\alpha$ -accompanied fission), are multiplied by a factor of 20

for the binary (ternary) case. The widths of the fitted curves were  $9.5 \pm 0.3$  ( $9.1 \pm 0.2$ ) units fwhm, in close agreement with [5, 6]. Thus, comparison of the spectra for both fission modes in the present experiment confirms convincingly the conclusion from former works [5, 6] that the strong enhancement of  $\gamma$ -rays at these high energies and near the mass symmetry is a peculiarity of the decay of equilibrated fragments around the double-magic shell closure  $N = 82$  ( $Z = 50$ ). Taking, for binary fission, an average value of  $A = 131.5 \pm 0.5$  from the present work and from [6] ( $A = 131.8$ ) and assuming that about 0.5 neutrons are emitted from these nuclei prior to  $\gamma$  decay [18], we obtain  $A = 131$  as the most probable fragment mass emitting these particular  $\gamma$ -rays. The corresponding average nuclear charge  $\bar{Z} = [(98/252) \cdot 131 - 0.3]$  is 50.6, and accordingly  $\bar{N} = 80.4$  [18]. So, fragments with  $A = 131$  are, on average, slightly closer to the magic proton number  $Z = 50$  than to the nearby  $N = 82$  closed neutron shell.

#### 4 Summary and conclusions

The high-energy  $\gamma$ -ray component was measured for the first time in the  $\alpha$ -particle accompanied fission mode of  $^{252}\text{Cf}$ . We found this bump in the  $\gamma$  spectrum to be equally pronounced in binary and  $\alpha$ -accompanied fission. Analysis of the fragment mass dependence of the mean  $\gamma$ -ray multiplicity in both modes, in the energy interval from 4 to 8 MeV, clearly identifies the enhancement of  $\gamma$ -ray yield at these high energies to be a peculiarity of the decay of fragments around the double-magic shell closure  $N = 82$  ( $Z = 50$ ), confirming the conclusions from [5, 6]. In fact, statistical model calculations

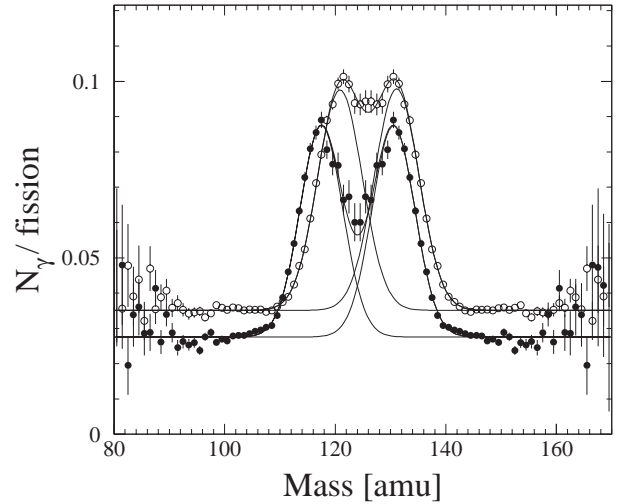


**Fig. 4.** Gamma yield  $N_\gamma$ , as a function of primary fragment mass, integrated over the  $\gamma$ -energy range from 4 to 8 MeV, for binary (open points) and  $\alpha$ -accompanied fission (full points).  $N_\gamma$  is normalized to the number of fission events in the respective mass split. Gaussian curves fitted to the data are indicated by dotted lines

presented in [6] could attribute the  $\gamma$ -ray bump to the strongly reduced level density of these nuclei in the relevant region of excitation energy. On the other hand, theoretical models [3, 4] that have predicted giant shape oscillations as a possible source of the  $\gamma$ -rays in question are contradicted by the experimental results. Also, accounts based on the emission of “relaxation  $\gamma$ ’s” when strongly deformed fragments near symmetry, as described by the super-long fission channel in the Brosa model [20], relax to their ground states, cannot be confirmed. These possible sources of  $\gamma$  emission in fission may probably be observed more favourably in the fission of actinides much lighter than  $^{252}\text{Cf}$  where the mass symmetry is farther away from the mass region around  $A = 132$ .

This work forms part of the PhD Thesis of P. Singer, TH Darmstadt (1997), and was supported in parts by the BMBF (06DA461 and 06TU669). The authors are indebted to F. Gönnenwein and E. Kankeleit for many stimulating discussions.

#### References

1. Hamilton J.H. et al., Progr. Part. Nucl. Phys. **35**, (1995) 635
2. Glässel P., Schmid-Fabian R., Schwalm D., Habs D., and v. Helmolt H.U., Nucl. Phys. **A502** (1989) 315c
3. Bartel J., Boose K., Dietrich K., Pomorski K., and Richert J., Z. Phys. **A339** (1991) 155
4. Pomorski K., Richert J., Bartel J. and Dietrich K., Z. Phys. **A345** (1993) 311
5. Fitzgerald J.B., Habs D., Heller F., Reiter P., Schwalm D., Thirolf P., and Wiswesser A., Z. Phys. **A355** (1996) 401
6. Hotzel A., Thirolf P., Enders Ch., Schwalm D., Mutterer M., Singer P., Klemens M., Theobald J.P., Hesse M., Gönnenwein F., and v.d. Ploeg H., Z. Phys. **A356** (1996) 299
7. Budtz-Jørgensen C., and Knitter H.H., Nucl. Phys. **A490** (1988) 307
8. Singer P., Kopach Yu., Mutterer M., Klemens M., Hotzel A., Schwalm D., Thirolf P., and Hesse M., Proc. “Third International Conference on Dynamical Aspects of Nuclear Fission - DANF96”, 30.8. - 4.9.1996, Casta Papiernicka, Slovakia, in press

9. Mutterer M. and Theobald J.P., in "Nuclear Decay Modes", Poenaru D.N. (Ed.), IOP Publ., Bristol, England (1996), Chap. 12
10. Wagemans C., in "The Nuclear Fission Process", Wagemans C. (Ed.), CRC Press, Boca Raton, Florida, USA (1991), Chap. 12
11. Metag V., Lecture Notes in Physics **178** (1983) 163
12. Mutterer M., Singer P., Kopach Yu., Klemens M., Hotzel A., Schwalm D., Thirof P., and Hesse M., Proc. "Third International Conference on Dynamical Aspects of Nuclear Fission - DANF96", 30.8. - 4.9.1996, Casta Papiernicka, Slovakia, in press
13. Hotzel A., Diploma Thesis, MPI für Kernphysik, Heidelberg (1994)
14. Heeg P., Mutterer M., Pannicke J., Schall P., Theobald J.P., and Weingärtner K., Proc. Conf. on 50 Years with Nuclear Fission (Gaithersburg, MD 1989), Behrens J.W., and Carlson A.D. (Eds.), American Nuclear Society, La Grange Park, IL, USA (1989) p. 299
15. Schmitt H.W., Kiker W.E., and Williams C.W., Phys. Rev. **137** (1965) B837
16. Düring I., PhD Thesis, TU Dresden (1993)
17. Alkhazov I.D., Kuznetsov A.V., and Shpakov V.I., Report RI-225 (1991), Atominform, Moscow
18. Wahl A.C., At. Data and Nucl. Data Tables **39** (1988) 1
19. Lang W.D. and Walsh R.L., Nucl. Instr. and Meth. **200** (1982) 389
20. Brosa U., Großmann S., and Müller A., Phys. Reports **197** (1990) 167

This article was processed by the author using the L<sup>A</sup>T<sub>E</sub>X style file *pljour2* from Springer-Verlag.